

Supplementary Materials of Encoder-decoder based image transformation approach for integrating precipitation forecasts

Hirotaka Hachiya

HHACHIYA@WAKAYAMA-U.AC.JP

Graduate School of Systems Engineering, Wakayama University/Center for AIP, RIKEN

Yusuke Masumoto

MASUMOTO.YUSUKE@G.WAKAYAMA-U.JP

Graduate School of Systems Engineering, Wakayama University/Center for AIP, RIKEN

Yuki Mori

MORI.YUKI-03@FUJITSU.COM

Numerical Prediction Development Center, Japan Meteorological Agency/Fujitsu Limited

Naonori Ueda

NAONORI.UEDA@RIKEN.JP

Center for AIP, RIKEN

Editors: Vineeth N Balasubramanian and Ivor Tsang

1. More details of experimental settings

Table 1: The initial time (INIT) and forecast time (FT) τ for each guidance, LFM, MSM and GSM. INIT and FT are the time of forecast generated and of the forecast targeting, respectively.

guidance	initial time (INIT)	forecast time (FT) τ [h]
LFM guidance	0:00, 3:00, 6:00, ..., 21:00UTC	3, 6, 9
MSM guidance	0:00, 3:00, 6:00, ..., 21:00UTC	3, 6, 9, ..., 39
GSM guidance	0:00, 6:00, 12:00, 18:00	6, 9, 12, 15, ..., 45

The details of the initial time (INIT) and forecast time (FT) of each guidance forecast, LFM, MSM, and GSM, are depicted in Table 1. INIT and FT are the time of the forecast generated and of the forecast targeting, respectively. As the table shows, GSM has different INIT and FT from the ones of LFM and MSM. To align the FT of all guidance forecasts among LFM, MSM, and GSM, we use past forecasts of GSM with INIT-6 or INIT-3 as follows:

- INIT-6 for 0:00, 6:00, 12:00 and 18:00UTC since no FT $\tau = 3$ exists in GSM
- INIT-3 for 3:00, 9:00, 15:00 and 21:00UTC since no GSM forecast exists

In addition, the evaluation region in the experiments is the land and coast of Japan corresponding to the grid points of 1 to 3 values in Fig. 1.

2. More details of Bayesian average and our proposed method iTraFI

Logistic regression model $b(\cdot)$ and weight W_k of mixture model in Eq. 5 in the manuscript are optimized using the recent past 30 days of data $\{F, Y\}$ based on the study ([Sloughter et al. \(2007\)](#)).

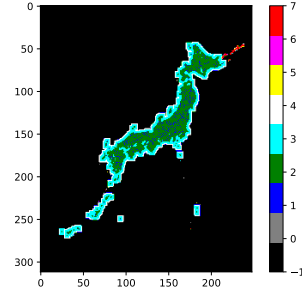


Figure 1: Forecast target area corresponding to the land and coast of Japan. In the experimental evaluation, grid points with the value of 1 to 3 are used.

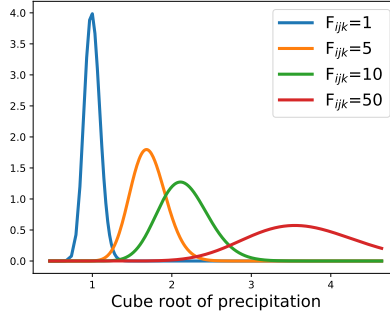


Figure 2: Examples of gamma distribution $g_k(\cdot)$ in Eq. 4 in the manuscript when parameters are set at $\mathbf{b} = (0, 1)$ and $\mathbf{c} = (0, 0.01)$. The x-axis is seen as the cubic root of the true value of precipitation from 0 to 100 [mm].

The parameters of the gamma distribution $g_k(\cdot)$ in Eq. 4 in the manuscript are tuned manually at $\mathbf{b} = (0, 1)$ and $\mathbf{c} = (0, 0.01)$ respectively, so that the probability density is high when the forecast F_{ijk} is close to the true value Y_{ij} as shown in Fig 2.

The details of operations at each layer of iTraFI (Fig. 2 in the manuscript) are described in Table 2. The number of channels of the feature map at each layer is set to the value to a multiple of $N_{\text{base}} = 20$. The embedding process of the information of FT τ (see Sec. 3.4 in the manuscript) is applied to the feature map Z , the output of conv5_2 and is indicated by mask_map operation.

3. Additional examples of forecasts

Fig. 3 depict true and forecasted precipitation generated by LFM-, MSM-, GSM-guidance, arithmetic average, Bayesian average, U-Net based regression and classification, and our proposed proposed method on August 15th 0:00 UTC for FT $\tau = 6$ in 2018 respectively.

Table 2: Details of each layer of U-Net in Fig. 2 in the manuscript. N_{in} and N_{base} are the number of channels of the input image X and the base number of channels of the feature map, respectively. conv, max_pool, batch_norm, upsample, relu, and softmax indicate the operations of 2d convolution, max-pooling, batch normalization, upsampling, ReLU, and sigmoid, respectively. All operation is done with the stride of 1×1 . concat and map_apply indicate the operation of the concatenate of the feature maps between encoder and decoder, i.e., skip-connection in Fig. 2 in the manuscript and applying the mask for the FT embedding (sec. 3.4 in the manuscript) respectively. Note that up-convolution in Fig. 2 in the manuscript is realized by a pair of up sampling and convolution operations.

Layer name	Channels	Kernel size			
input	N_{in}	-			
conv1_1	N_{base}	3×3			
conv1_2	N_{base}	3×3			
batch_norm	N_{base}	-			
max_pool	N_{base}	2×2			
conv2_1	$N_{\text{base}} \times 2$	3×3			
conv2_2	$N_{\text{base}} \times 2$	3×3			
batch_norm	$N_{\text{base}} \times 2$	-			
max_pool	$N_{\text{base}} \times 2$	2×2			
conv3_1	$N_{\text{base}} \times 4$	3×3			
conv3_2	$N_{\text{base}} \times 4$	3×3			
batch_norm	$N_{\text{base}} \times 4$	-			
max_pool	$N_{\text{base}} \times 4$	2×2			
conv4_1	$N_{\text{base}} \times 8$	3×3			
conv4_2	$N_{\text{base}} \times 8$	3×3			
map_apply	$N_{\text{base}} \times 8$	-			
batch_norm	$N_{\text{base}} \times 8$	-			
conv5_1	$N_{\text{base}} \times 16$	3×3			
conv5_2	$N_{\text{base}} \times 16$	3×3			
map_apply	$N_{\text{base}} \times 16$	-			
batch_norm	$N_{\text{base}} \times 16$	-			
			upsample	$N_{\text{base}} \times 16$	2×2
			conv6_0	$N_{\text{base}} \times 8$	3×3
			concat with conv4_2	$N_{\text{base}} \times 16$	-
			conv6_1	$N_{\text{base}} \times 8$	3×3
			conv6_2	$N_{\text{base}} \times 8$	3×3
			upsample	$N_{\text{base}} \times 8$	2×2
			conv7_0	$N_{\text{base}} \times 4$	3×3
			concat with conv3_2	$N_{\text{base}} \times 8$	-
			conv7_1	$N_{\text{base}} \times 4$	3×3
			conv7_2	$N_{\text{base}} \times 4$	3×3
			batch_norm	$N_{\text{base}} \times 4$	-
			upsample	$N_{\text{base}} \times 4$	2×2
			conv8_0	$N_{\text{base}} \times 2$	3×3
			concat with conv2_2	$N_{\text{base}} \times 4$	-
			conv8_1	$N_{\text{base}} \times 2$	3×3
			conv8_2	$N_{\text{base}} \times 2$	3×3
			batch_norm	$N_{\text{base}} \times 2$	-
			upsample	$N_{\text{base}} \times 2$	2×2
			conv9_0	N_{base}	3×3
			concat with conv1_2	$N_{\text{base}} \times 2$	-
			conv9_1	N_{base}	3×3
			conv9_2	N_{base}	3×3
			conv9_3	N_{base}	3×3
			conv9_4	N_{ft}	3×3

References

- J. M. Sloughter, A. E. Raftery, T. Gneiting, and C. Fraley. Probabilistic quantitative precipitation forecasting using bayesian model averaging, 2007.

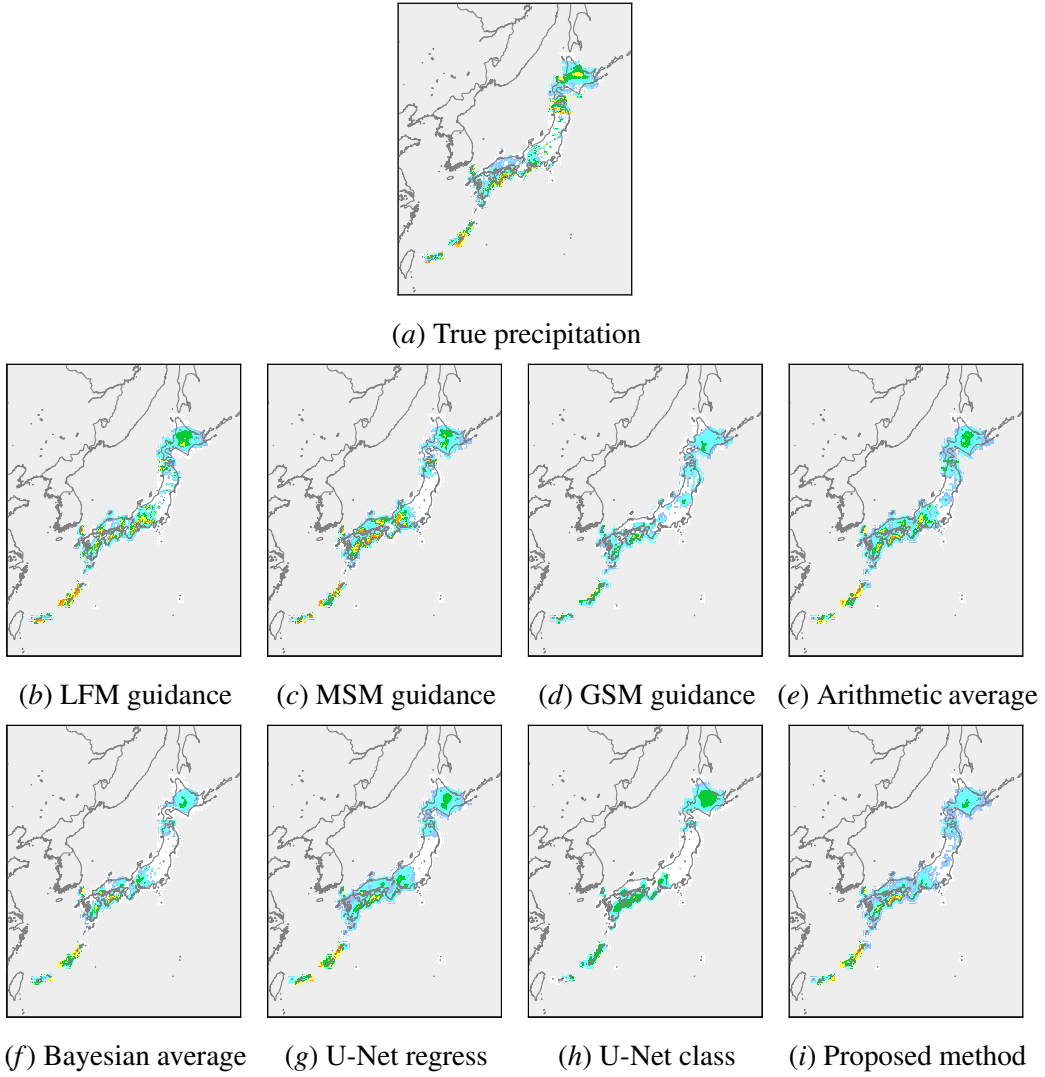


Figure 3: True and forecasted precipitation drawn on a map. The forecasts are generated by LFM-, MSM- and GSM-guidance, arithmetic and Bayesian average, U-Net based regression and classification, and iTraFI, on Aug. 15th, 0:00UTC, 2018 for FT $\tau = 6$.

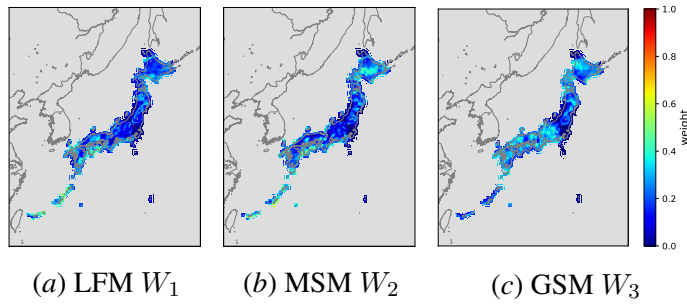


Figure 4: Weights W_k for each guidance, drawn on a map. These weights are generated by proposed method, iTraFI, on Aug. 15th, 0:00UTC, 2018 for the FT $\tau = 6$.